



Bmi1 regulates human glioblastoma stem cells through activation of differential gene networks in CD133+ brain tumor initiating cells

Parvez Vora^{1,2} · Mathieu Seyfrid^{1,2} · Chitra Venugopal^{1,2} · Maleeha A. Qazi^{1,3} · Sabra Salim³ · Ruth Isserlin⁴ · Minomi Subapanditha¹ · Erin O'Farrell^{1,3} · Sujeivan Mahendram^{1,2} · Mohini Singh³ · David Bakhshinyan^{1,3} · Chirayu Chokshi^{1,3} · Nicole McFarlane^{1,2} · Anna Dvorkin-Gheva⁵ · Kevin R. Brown⁴ · Naresh Murty² · Jason Moffat⁴ · Gary D. Bader⁴ · Sheila K. Singh^{1,2,3}

Received: 9 October 2018 / Accepted: 10 May 2019
© Springer Science+Business Media, LLC, part of Springer Nature 2019

Abstract

Purpose Glioblastoma (GBM) is the most aggressive adult brain cancer, with a 15 month median survivorship attributed to the existence of treatment-refractory brain tumor initiating cells (BTICs). In order to better understand the mechanisms regulating the tumorigenic properties of this population, we studied the role of the polycomb group member BMI1 in our patient-derived GBM BTICs and its relationship with CD133, a well-established marker of BTICs.

Methods Using gain and loss-of-function studies for *Bmi1* in neural stem cells (NSCs) and patient-derived GBM BTICs respectively, we assessed in vitro self-renewal and in vivo tumor formation in these two cell populations. We further explored the BMI1 transcriptional regulatory network through RNA sequencing of different GBM BTIC populations that were knocked down for *Bmi1*.

Results There is a differential role of BMI1 in CD133-positive cells, notably involving cell metabolism. In addition, we identified pivotal targets downstream of BMI1 in CD133+ cells such as integrin alpha 2 (ITGA2), that may contribute to regulating GBM stem cell properties.

Conclusions Our work sheds light on the association of three genes with CD133-BMI1 circuitry, their importance as downstream effectors of the BMI1 signalling pathway, and their potential as future targets for tackling GBM treatment-resistant cell populations.

Keywords Glioblastoma · Patient-derived brain tumor initiating cells · BMI1 · CD133

Electronic supplementary material The online version of this article (<https://doi.org/10.1007/s11060-019-03192-1>) contains supplementary material, which is available to authorized users.

✉ Sheila K. Singh
ssingh@mcmaster.ca

- ¹ Stem Cell and Cancer Research Institute, McMaster University, 1280 Main Street West, Hamilton, ON L8S 4K1, Canada
- ² Department of Surgery, McMaster University, Hamilton, ON, Canada
- ³ Department of Biochemistry and Biomedical Sciences, McMaster University, Hamilton, ON, Canada
- ⁴ Donnelly Centre and Department of Molecular Genetics, University of Toronto, Toronto, ON, Canada
- ⁵ Department of Pathology and Molecular Medicine, McMaster University, Hamilton, ON, Canada

Introduction

Bmi1 (B cell-specific Moloney murine leukemia virus insertion site-1) is a member of the highly conserved polycomb group (PcG) gene family, and acts as a transcriptional repressor of multiple genes, including genes that determine proliferation and differentiation of cells throughout development [1–5]. BMI1 is essential for the self-renewal and proliferation of both normal neural and hematopoietic stem cells [6–11]. It is a key component of PRC1, as the loss of Ring1a or M33 from the complex does not affect self-renewal of neurospheres, while loss of *Bmi1* alone causes clear deficits in self-renewal [8]. Indeed, BMI1 deficiency has a negative effect on self-renewal, proliferation, and differentiation potential in multiple cell types including normal murine neural stem cells (NSCs), hematopoietic stem cells (HSCs) and cancer stem cells (CSCs) both in vitro and

in vivo [4, 6, 8–10, 12]. Within normal NSCs, BMI1 plays a role in regulating self-renewal and proliferation [12], and in decreasing differentiation, thus making it an excellent target for potential deregulation within cancer [13, 14].

BMI1 was first identified as an oncogene which cooperated with the oncogene *c-myc* within murine lymphomagenesis [15, 16]. BMI1 has since been shown to be often overexpressed in multiple cancers including leukemia, hepatocellular carcinoma, laryngeal carcinoma, lung cancer, breast cancer, colon cancer, and brain tumors such as medulloblastoma and glioblastoma (GBM) [4, 6, 13, 17–23]. Interestingly, within GBM cells, overexpression of *Bmi1* is not associated with gene amplification, therefore, it is most likely the result of increased transcription, notably by miRNAs [24, 25].

Further studies have indicated that *Bmi1* knockdown in GBM cells inhibits cell proliferation and self-renewal in vitro through increased apoptosis and differentiation, independent of a functional *INK4A/ARF* locus, suggesting alternative pathways for *Bmi1* repression [6]. By combining ChIP-seq with in vivo RNAi screening in mouse and human neural progenitors and GBM stem cells, Gargiulo et al. [26] discovered that BMI1 is important in the cellular response to the transforming growth factor- β /bone morphogenetic protein (TGF- β /BMP) and endoplasmic reticulum (ER) stress pathways, in part converging on the Atf3 transcriptional repressor. The identification of functional tumor suppressor targets in this work, including Atf3 and Cbx7, highlights the multiple p16(INK4a)/p19(ARF)-independent functions for BMI1 in development and cancer. However, much work still remains to determine other *Bmi1* regulatory mechanisms and pathways which may influence cancer progression.

BMI1 has most recently been cited as a marker of progression in many cancer models [27, 28], and most strikingly, a BMI1-driven gene signature has been identified through a mouse/human comparative translational genomics approach and validated in numerous human cancers [29]. This 11-gene signature representing a conserved BMI1-driven transcriptional network displays a stem cell-resembling signature, and reliably predicts recurrence, poor treatment response, metastatic potential and death from cancer in 11 clinical cancer subtypes.

The inevitable development of therapy resistance and disease relapse observed in GBM, the most aggressive and lethal human brain tumor, may be explained by the persistence of brain tumor initiating cell (BTIC) populations that evade both chemo- and radiotherapy [21, 30]. A novel stem cell model of recurrent GBM [31] revealed that chemoradiotherapy increased the expression of genes that drive BTICs self-renewal, including *Sox2* and *Bmi1*, and another study found that BMI1 confers radioresistance to normal NSCs and BTICs through recruitment of the DNA damage response machinery [32]. Enhanced BMI1 expression

in BTICs may thus allow these cells to evade therapy to form a disease reservoir that may drive disease recurrence and relapse.

The current study investigates the role of BMI1 in regulating BTICs function in GBM through knockdown of *Bmi1* in BTIC populations and overexpression of *Bmi1* in normal human NSC populations. Furthermore, and in keeping with previous investigations [6], we sought to explore the relationship between BMI1 and CD133, an established NSC- and BTIC-associated marker [33]. Through RNA sequencing of CD133+ and CD133– cell populations knocked down for *Bmi1*, we elucidate novel *Bmi1*-driven gene regulatory networks that may contribute to therapy resistance driven by BTIC populations, particularly with respect to novel gene networks elucidated in the self-renewing CD133+ cell population. In addition, we report a CD133-dependent BMI1 signature, which delineates BMI1 transcriptional influence and improves knowledge of its complex circuitry.

Results

***Bmi1* overexpression in human NSCs induces increased self-renewal and proliferation in vitro, but is not sufficient to drive tumor formation in vivo**

In multiple cancer models, BMI1 is an oncoprotein pre-requisite for transformation, metastatic migration, and maintenance of malignancy [8, 21, 29, 34, 35]. To determine if BMI1 expression is necessary and sufficient to drive the transformation of NSCs to BTICs, we undertook lentiviral transduction of a *Bmi1*-overexpressing (OE-Bmi) construct into three different primary human fetal NSC lines. After transduction, GFP-expressing OE-BMI1 NSCs (Supplementary Fig. S1A and B) were further sorted by flow cytometry by GFP and CD133 expression. As previously reported, CD133(+) NSCs have a higher level of self-renewal and proliferation, and *Bmi1*-overexpressing NSCs exhibit a higher self-renewal capacity (Fig. 1a, Supplementary Fig. S1C) in all lines, as well as increased proliferative ability for two out of three lines (Fig. 1b, Supplementary Fig. S1D), compared to control NSCs. This BMI1-mediated control of BTICs-associated features, in addition to the paradigm that glioma stem cells derive from transformed NSCs [36], led us to investigate whether *Bmi1* over-expression is necessary and sufficient for malignant transformation of NSCs. We therefore intracranially engrafted the OE-BMI1 NSC197 line into immunodeficient mice, as it displayed the highest increase in self-renewal among the NSC lines used. However, up to one million BMI1-OE NSCs intracranially transplanted into the right frontal lobes of adult NOD-SCID mice failed to generate brain tumors at 3 months post-engraftment (Supplementary Fig. S1E). To investigate if tumor formation

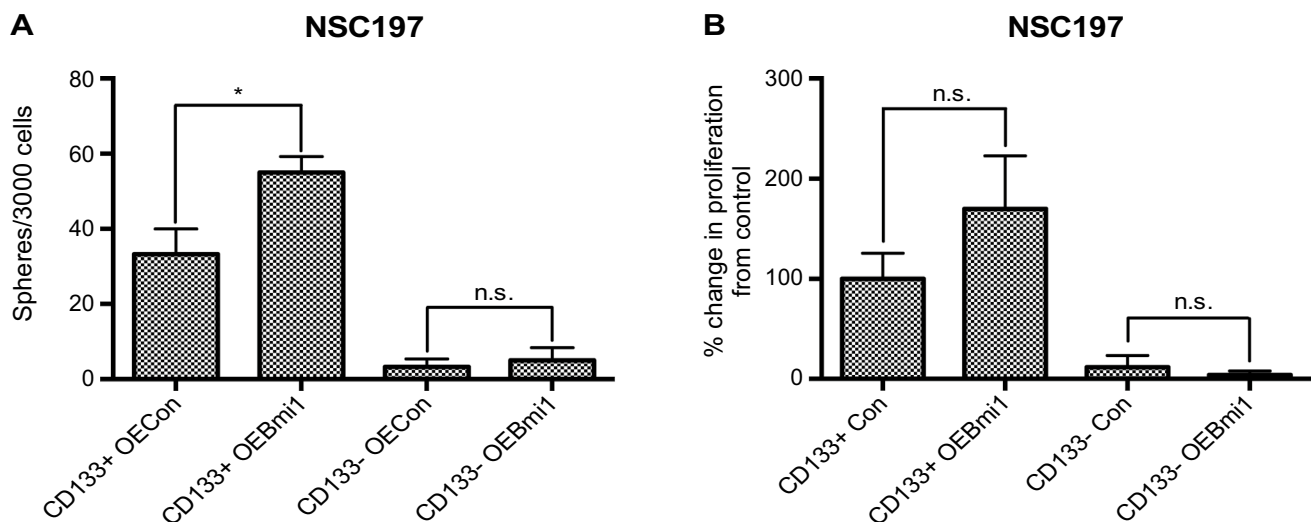


Fig. 1 Bmi1 overexpression in neural stem cell and progenitor cells (NSPCs) increases stemness. **a** Lentiviral vector-mediated Bmi1 overexpression (OEBmi1) leads to increased self-renewal and **b** increased

proliferative capacity in NSC197 line, when compared to control (OECon); * $p < 0.05$; n.s. non significant

could occur if Bmi1 was overexpressed in NSCs during early embryonic development, we performed in utero electroporation of BMI1-OE plasmids into the developing cerebral cortex of E14 fetal mouse brains, and tumor formation was evaluated after the pups were 2 months old (data not shown). Although we observed no tumor formation in mouse brains, it is possible that more prolonged *Bmi1* overexpression, or *Bmi1* overexpression combined with overexpression of cooperating oncogenes, may result in tumor initiation in the NSC compartment. Examination of adult mice brains revealed hydrocephalus in only BMI1-OE mice compared to controls (Supplementary Fig. S1E), which may result from tumor cells seeding the cerebrospinal fluid, but not reaching critical mass for tumor formation. Taken together, this data suggests that although *Bmi1* overexpression increases self-renewal and proliferation of NSCs in vitro, *Bmi1* overexpression alone is not sufficient to transform NSCs and initiate tumors, as observed in two different in vivo models.

***Bmi1* knockdown in BTICs results in decreased self-renewal, proliferation and migration in vitro and reduces tumor size and invasiveness in vivo**

We next sought to determine if *Bmi1* knockdown is sufficient to decrease the self-renewal and tumor-initiating capacity of BTICs. Stable Bmi1 knockdown using lentiviral plasmids-encoding shRNAs (Supplementary Fig. S2A–C) resulted in significantly decreased self-renewal (Fig. 2a, Supplementary Fig. S2D) and proliferation (Fig. 2b) of BTICs in vitro, and also resulted in decreased migratory capacity of BTICs (Fig. 2c and d). To evaluate effects on in vivo tumor-initiating potential, we performed intracranial xenotransplantation

of two different BTIC patient-derived lines transduced with shBmi1 or shLuc control vectors into NOD-SCID mice. Five weeks post-transplantation, shBmi1 cells displayed a reduced tumor size and invasiveness, compared to control cells (Fig. 2e and f), regardless of the number of cells injected (Supplementary Fig. S2E). This conferred significant extended survival to shBmi1-engrafted mice, compared to their shLuc counterpart (Fig. 2g).

Identification of CD133-specific BMI1 signatures in GBM BTICs

In order to further understand BMI1-associated gene regulation, we performed RNA sequencing on two different BTIC lines. Since we have previously demonstrated that BMI1 contributes to self-renewal in CD133+ populations, but regulates proliferation and cell fate determination in CD133– populations [37], we sought to explore the mechanism by which *Bmi1* gene dosage may regulate different aspects of tumorigenesis in CD133+ and CD133– cell compartments. We thus applied flow cytometry to sort control (shLuc) and shBmi1 cells into CD133+ and CD133– subpopulations and performed RNAseq on these populations (Fig. 3a).

Remarkably, the gene expression profile (up- and down-regulated genes) triggered by BMI1 silencing in CD133+ cells had little overlap with their CD133– counterparts (Fig. 3b). We analyzed levels of gene enrichment in shBMI1 CD133+ cells compared to shBMI1 CD133– cells, and clustered them into pathway associations and node-networks (Fig. 3c), which allowed the establishment of a comprehensive gene dataset enrichment map. Pathway nodal analysis

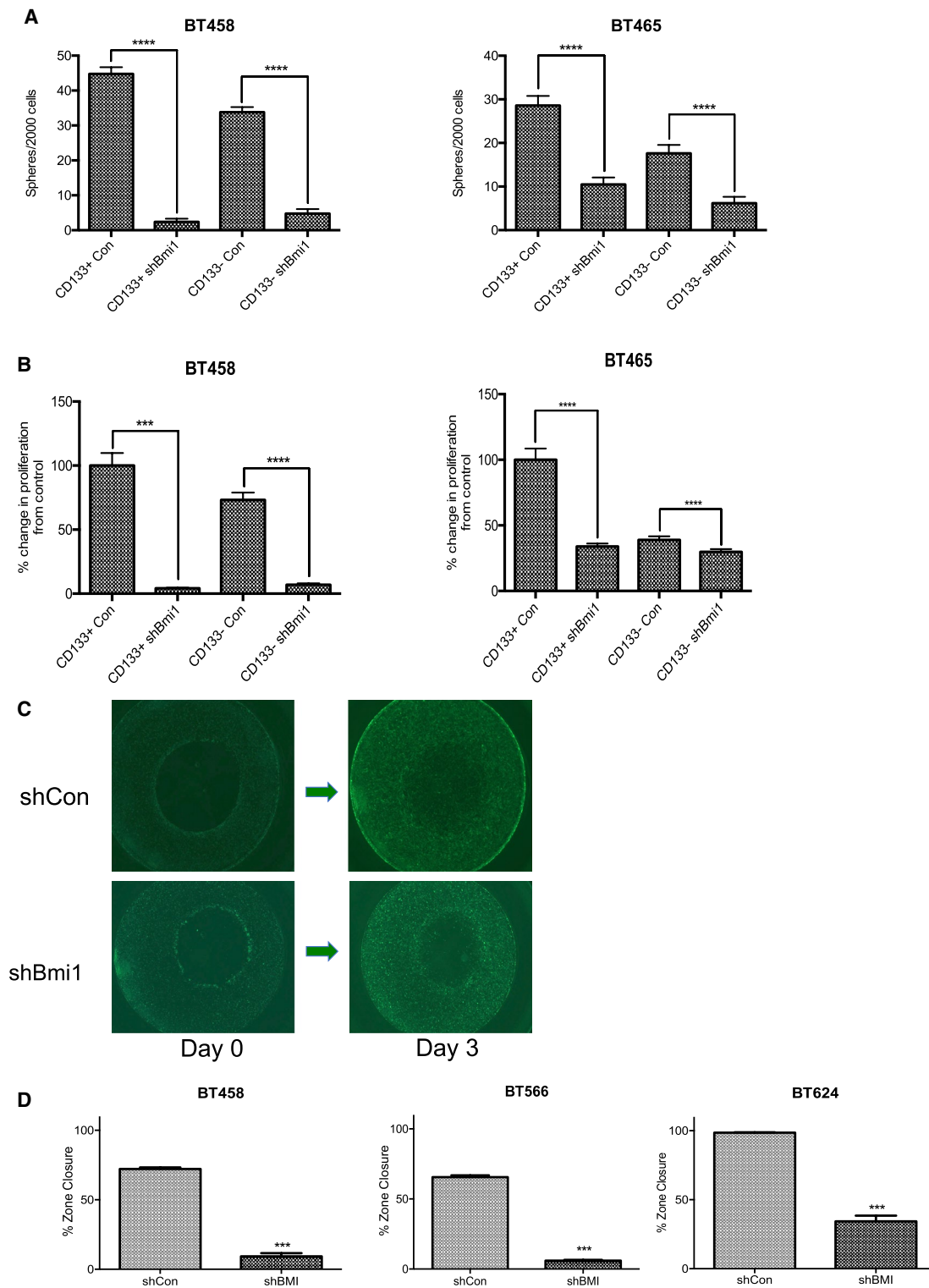


Fig. 2 Bmi1 knockdown affects CD133+ GBM cells by functionally reducing their sphere formation and proliferation capacities. **a** Lentiviral vector-mediated Bmi1 knockdown with shRNA leads to decreased in self-renewal and **b** proliferation in different BTIC populations. *** $p < 0.005$ and **** $p < 0.001$. **c** Representative images of BTICs in zone exclusion, migration assay. **d** Quantification of migration on different BTICs lines, where shBmi1 decreases their migration capacities. **e** CD133^{high} and CD133^{low} lines were transduced with shBmi1 or

shControl vector ex vivo and injected intracranially into NOD-SCID mice. Assessment of tumor formation five weeks post-transplantation reveals significantly decreased GBM tumor size and invasion in absence of Bmi1; $n = 5$ for each group. **f** Bmi1-silencing decreases sphere formation in BT428 cells. **f** Tumor area of mice xenografted with BT428 shCon/shBmi1, where shBmi1 engrafted cells are linked with a smaller tumor area; $n = 3$ for each group; * $p < 0.05$; **g** Kaplan–Meier curves for mice xenografted with BT241 shCon/shBmi1 ($n = 4$ for each group)

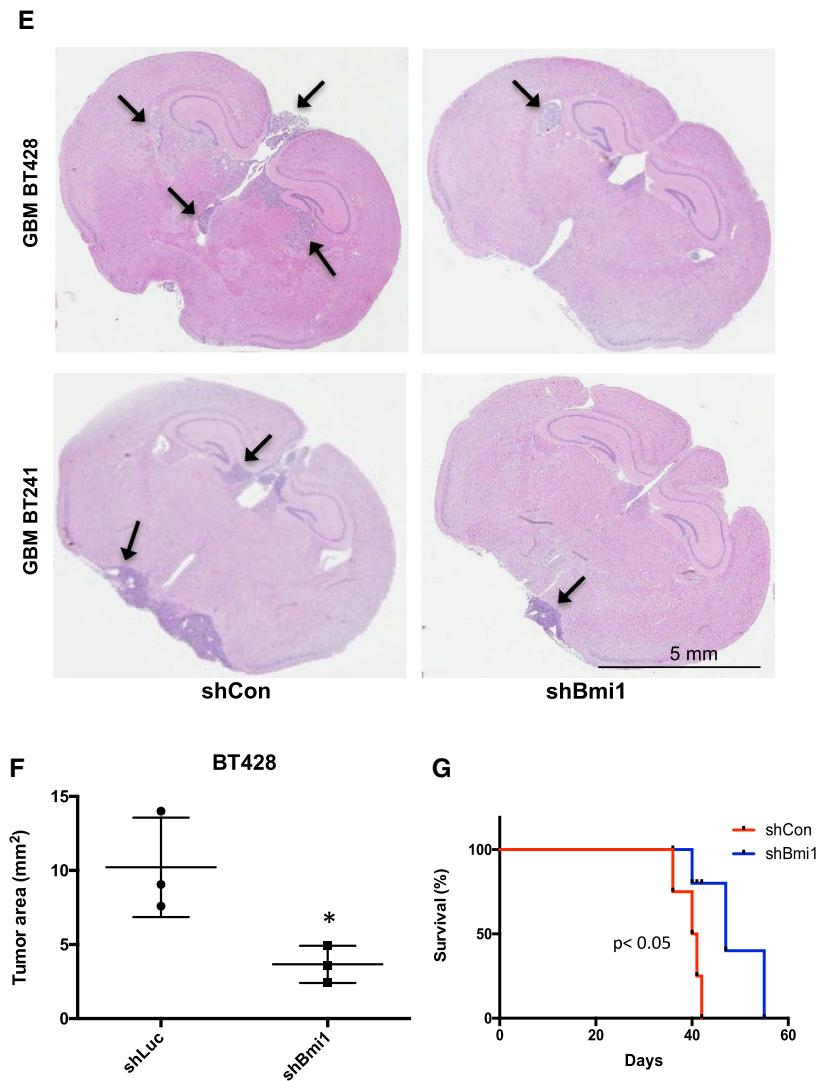


Fig. 2 (continued)

revealed a remarkable influence of BMI1 upon cell energetics in the CD133+ BTIC compartment (Fig. 3c, Supplementary Fig. S3A), as silencing *Bmi1* in CD133+ cells upregulates different cell metabolic pathways. In addition, CD133+ cells possess migration-linked capacities that rely on BMI1, as suggested by downregulation of different clusters (e.g. amoebial type cell migration, adherens junction focal substrate) (Fig. 3c).

We further refined our RNA sequencing results by probing the GSEA Msigdb C6 oncogene geneset, an oncogenic pathway-specific database (<https://software.broadinstitute.org/gsea/msigdb/genesets.jsp?collection=C6>) that further emphasises the differences in CD133 compartments after BMI1 knockdown (Supplementary Fig. S4 and S5). Our pathway analysis showed a strong dependency of BMI1 in CD133+ cells in invasion-related processes, such as

extracellular matrix organization and collagen metabolic processes (Fig. 3d, Supplementary Figs. S4A and S5A). Conversely, in CD133- cells, BMI1 appears to control the DNA replication machinery (transcription/translation) (Fig. 3e, Supplementary Figs. S4B and S5B), supporting the role of these cells in proliferative capacity. In addition, there is a correlation in CD133- cells between BMI1 and AP-1 (Fig. 3e), the latter being a transcription factor controlling proliferation and cell death, whose implication in BMI1 signaling pathway has been shown in carcinomas [38], but not so far in GBM.

We then chose to focus on genes not belonging to any of the above signaling pathways, searching for novel GBM-specific genes that may regulate self-renewal through BMI1. Among top differentially expressed genes markedly downregulated in CD133+ cells (Supplementary Fig. S6A), we identified ITGA2, FSTL1 and ALK, as having their

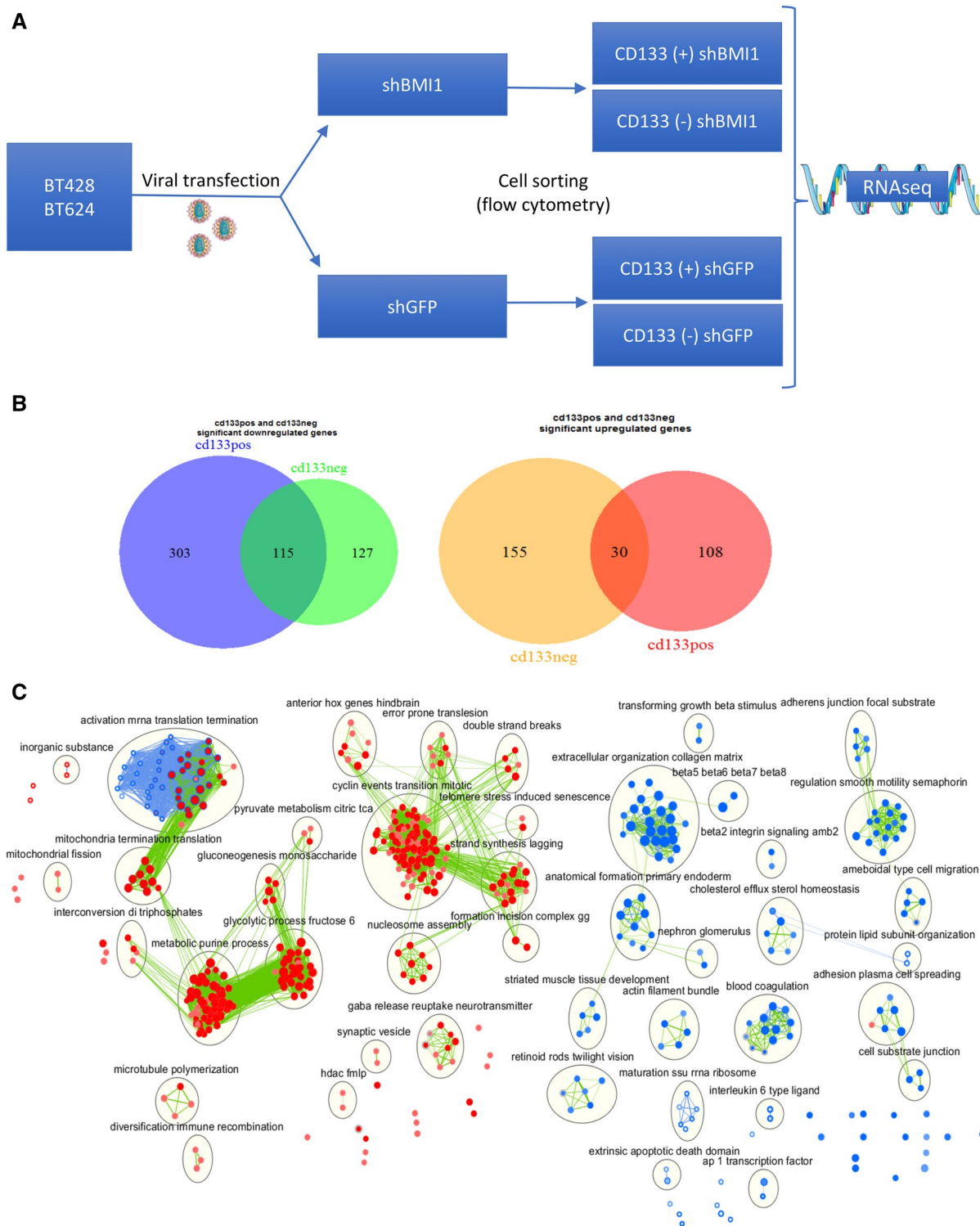


Fig.3 RNAseq of BMI1 silencing for CD133+ and CD133- cells in BTICs. **a** Workflow of the RNAseq; **b** schematic analysis of the overlap of increase/decreased genes expressions, in CD133+ (top) and CD133- (bottom) cells; **c** two dataset Enrichment map comparing the enrichments of CD133+ and CD133-. Node interior and green edges represent CD133+ results. Node border and blue edges represent CD133- results. Nodes with only blue edges are exclusively enriched in CD133-, nodes with only green edges are exclusively enriched in CD133+. Results showing the pathways enriched in genes dysregulated in the BMI1 knockout compared to control

(Blue sets are down-regulated in BMI1KD and red sets are up regulated in BMI1KD). (p-value<1.0, FDR<0.1, combined (constant=0.5) similarity>0.375). Clusters are annotated with the most frequent words from the set of node names (as calculated using clustermaker with MCL clustering (Morris et al. 2011) and WordCloud app with normalization factor=0.5 (Oesper et al. 2011) using the AutoAnnotate Cytoscape app; **d** and **e** representation of GSEA Msigdb C6 genesets (<https://software.broadinstitute.org/gsea/msigdb/genesets.jsp?collection=C6>) enrichment plot in **d** CD133-positive and **e** CD133-negative up or downregulated genes

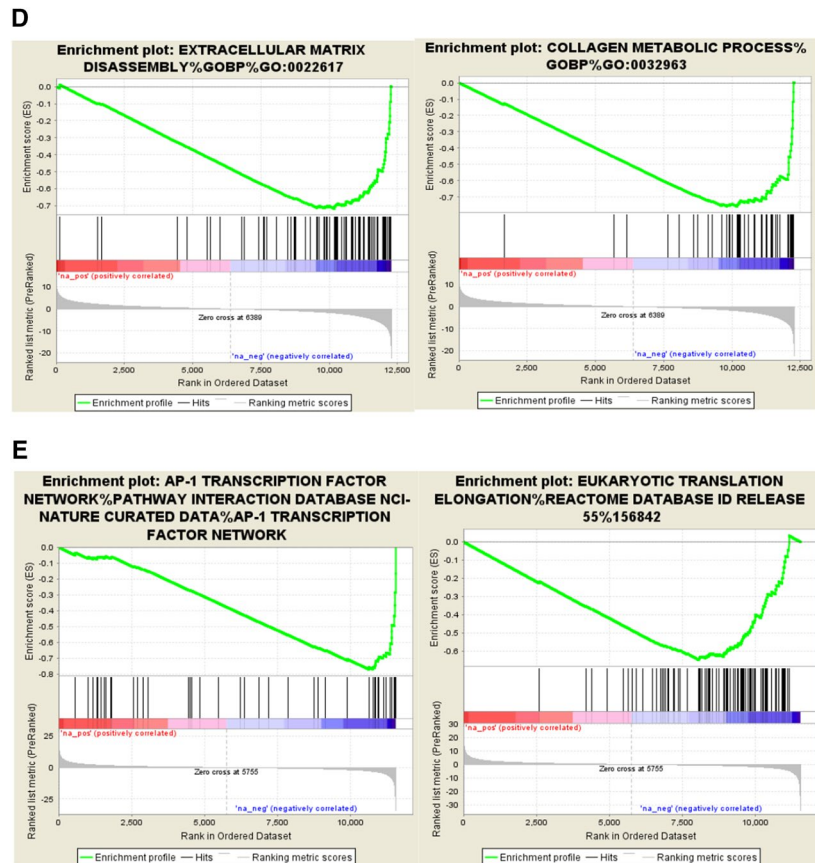


Fig. 3 (continued)

expression levels decreased in CD133+ cells with *Bmi1* silencing. We further confirmed by RT-qPCR that silencing of BMI1 downregulates these three genes (Fig. 4a). Finally, we individually silenced them using short-hairpin RNA (Supplementary Fig. S6B), which resulted in a dramatic impairment of BTIC self-renewal, but not of their proliferation capacities (Fig. 4b and c), underscoring their potential importance in the BMI1-mediated stemness and tumorigenicity.

Discussion

Despite decade-long extensive investigation of GBM, most of the complexity and pathway interdependency of this aggressive brain cancer remains unknown. Escape from therapy has been linked with the CD133+ GBM cell population [39], suggesting that molecular targeting of this cell subset could lead to significant clinical improvement. One way GBM can leverage adaptation to its environment is through epigenetic modulation of genes [40]. This reprogramming is orchestrated by different key factors, among them the chromatin-modifying Polycomb-group gene *Bmi1*

[6, 24, 41]. We previously identified CD133+ cells as the population in which *Bmi1* regulates self-renewal, in a cell-context dependent manner [37]. The scope of the current work was to decipher the molecular ties between BMI1 and CD133 in an aggressive cellular sub-population of GBM, namely BTICs.

We first addressed whether *Bmi1* overexpression itself can trigger a malignant switch in NSCs, which could help our understanding of tumor initiation. Although *Bmi1* modulation clearly affected self-renewal and proliferation of NSCs in vitro, it was not sufficient for transformation and tumor formation in vivo, in adult or embryonic NSCs. One reason might be the need for a favorable chromatin configuration to fully recapitulate the epigenetic landscape necessary for tumorigenesis [42]. Indeed, another member of the Polycomb family, EZH2, can contribute to create a H3K27 methylation pattern appropriate for BMI1-mediated gene silencing [43] and BMI1 upregulation has been recently shown to be essential in a H3K27-methylated population of pediatric gliomas [44], further underscoring its role in epigenetic regulation, and corresponds with the recent suggestion of co-targeting both BMI1 and EZH2 to target differing GBM micro-environments [45].

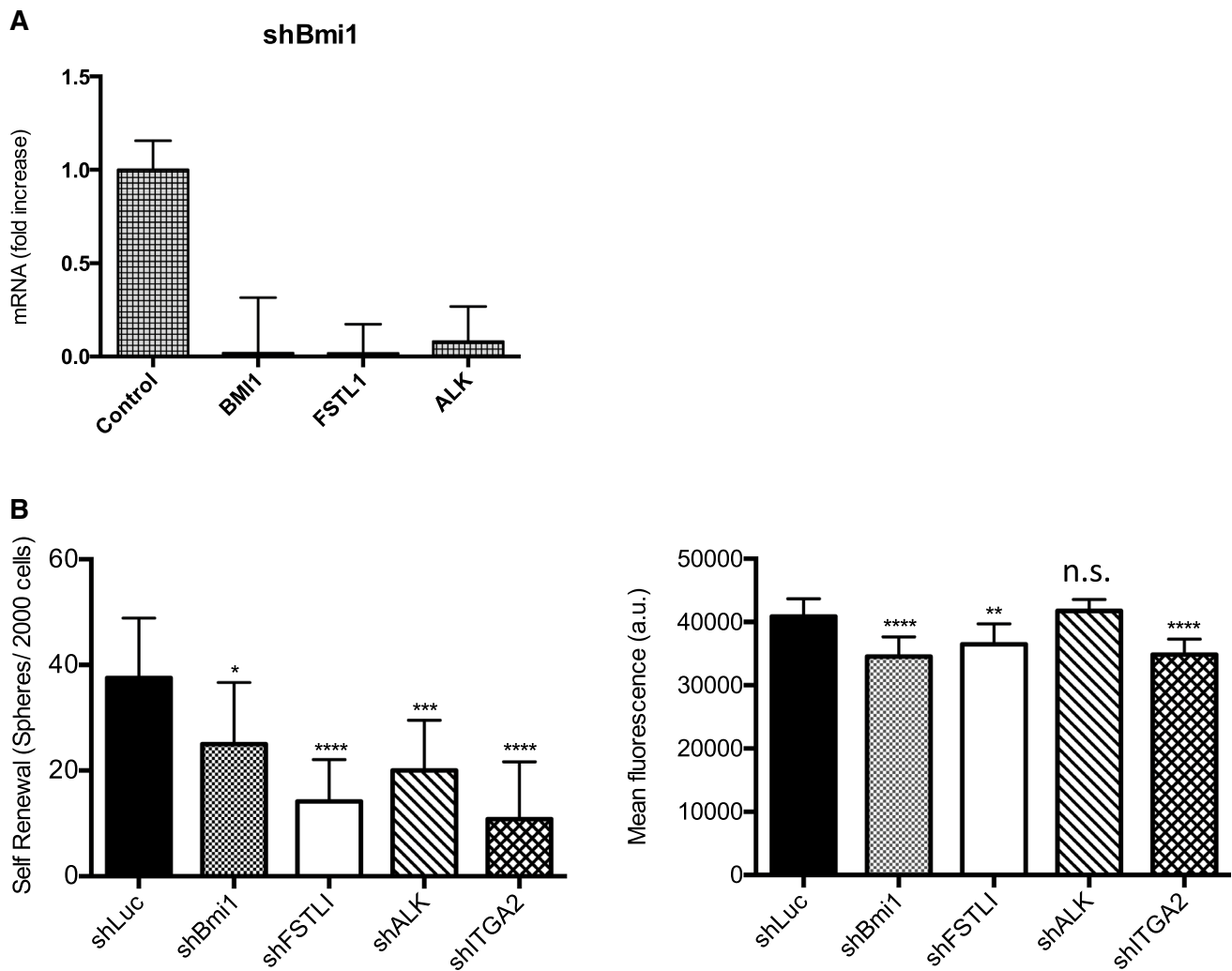


Fig. 4 Validation of the RNAseq hits by RT-qPCR in BT458 line. **a** mRNA expression of BMI1, FSTL1 and ALK is decreased in shBmi1 cells; results are normalized on 28 s rRNA expression, and compared towards their respective levels in control cells **b** short-hairpin knock-

down of Bmi1, FSTL1, ALK and ITGA2 all decrease self-renewal and **c** on proliferative capacities of BT458, as measured by Presto-Blue assay. * $p < 0.05$; ** $p < 0.01$; *** $p < 0.005$; **** $p < 0.001$; n.s. non significant

Finally, concomitant downregulation of downstream tumor suppressors [26], as well as modulation of upstream modulators of PCR1 and PCR2, such as miRNAs [46], are also probably needed to recapitulate a complete malignant transformation of NSCs.

Next, we highlighted the importance of BMI1 in actively maintaining BTIC function (stemness, proliferation and migration) in CD133+ cells, although we cannot exclude that this maintenance is additionally controlled by other oncogenic signals [19]. To further investigate BMI1-dependent genes in CD133+ cells versus CD133- cells, we analyzed their transcriptomes under *Bmi1* silencing. Gene clustering analysis revealed distinct tumor-propagating roles for BMI1, depending on the cell's CD133 status. Notably, BMI1 has control over key metabolism-associated processes (gluconeogenesis, TCA cycle) only

in CD133+ populations. Previous work already pinpointed the involvement of BMI1 in glucose regulation in normal cells [47], but to our knowledge this is the first time it has been implicated in GBM. As metabolic flexibility is vital for GBM cells to survive in a low-glucose, hypoxic tumor microenvironment [48], our results suggest an unstudied cooperation of BMI1 and CD133 in GBM adaptability to hostile conditions.

In addition, our screen showed the involvement of BMI1 in migration/invasion of CD133+ cells. Evidence gathered from other cancers has already shown that BMI1 and CD133 participate in epithelial-to-mesenchymal transition (EMT) [49]; this reflects the dual identity of stem and invading cells, as well as the metabolic switch necessary to adapt to or escape from the aggressive microenvironment in which GBM thrives. Moreover, CD133 expression is linked to the TCGA Mesenchymal

GBM subclass [50], which harbours both higher cell metabolism and migration potential [51].

Lastly, we validated our screen by silencing three gene candidates whose expression is dependent on BMI1, namely ALK, FSTL1 and ITGA2, and observed that their absence dramatically impaired self-renewal (but not proliferation) of GBM BTICs. ALK is a kinase mainly known for its protumorigenic involvement in lymphoma [52] and non-small cell lung cancer [53], and ALK-targeting therapies are currently under development in GBM [54]. FSTL1 has been associated with poor prognosis in GBM patients [55], and acts on the TGF β pathway by regulating Smad phosphorylation [56], illustrating the known influence of BMI1 on TGF β [26]. Finally, integrin alpha 2 (ITGA2) has been attributed with pro- or anti-invasion/migration properties in, among others, breast [57] and prostate cancer models [58], but has not been extensively studied in GBM yet. We believe these genes constitute potential candidates for the development of a multitargeting therapeutic strategy needed to induce GBM remission [59]. Moreover, regarding the hope created by the application of immunotherapies to GBM [60], ITGA2 could represent a co-target for a bispecific antibody targeting approach along with CD133, both being located at the cell surface of GBM BTICs.

To summarize, we investigated the role of BMI1 in GBM pathogenesis and its coordination of aggressive biological drivers, and unraveled the existence of a CD133-dependent BMI1-controlled pathway involved in metabolic plasticity and migration/invasion. In addition, we showed here for the first time the association of three genes with CD133-BMI1 circuitry, their importance as downstream effectors of the BMI1 signalling pathway and as such, their potential as future targets for tackling GBM treatment-resistant cell populations.

BMI1 can also be controlled post-translationally, notably by miR-128 [61], and additional proteomic investigation of the shift provoked by knockdown of BMI1 in BTIC populations depending on their CD133 status could bring further insights in the dynamics of the role of Bmi1 in different CD133 compartments. Advanced techniques such as single cell RNA seq would be useful in elucidating the oncogenic programs at the single cell level [44] and pinpoint the role of BMI1 in CD133+ versus CD133– populations at the clonal level. In addition, upcoming studies could examine the connection of other members of the polycomb repressor group with CD133, as well as determine at which level (transcriptional, translational, or post-translational) BMI1 exerts its effects on the CD133 positive BTIC population.

Material and methods

Dissociation and culture of primary GBM tissue

Human GBM samples were obtained from consenting patients, as approved by the Hamilton Health Sciences/McMaster Health Sciences Research Ethics Board. Samples

were dissociated in artificial cerebrospinal fluid containing 0.2 Wünsch unit/mL Liberase Blendzyme 3 (Roche), and incubated at 37 °C in a shaker for 15 min. The dissociated tissue was filtered through a 70 μ m cell strainer and collected by centrifugation (1500 rpm, 3 min). Tumor cells were resuspended in Neurocult complete media, a chemically defined serum-free neural stem cell medium (STEMCELL Technologies), supplemented with human recombinant epidermal growth factor (20 ng/mL; STEMCELL Technologies), basic fibroblast growth factor (20 ng/mL; STEMCELL Technologies), heparin (2 μ g/mL 0.2% Heparin Sodium Salt in PBS; STEMCELL technologies), antibiotic–antimycotic (10 mg/mL; Wisent), and plated on ultra-low attachment plates (Corning). Red blood cells were lysed using ammonium chloride solution (STEMCELL Technologies).

Propagation of BTICs

Neurospheres derived from minimally-cultured human GBM samples were plated on polyornithine-laminin coated plates for adherent growth. Adherent cells were replated in low-binding plates and cultured as tumorspheres, which were maintained as spheres upon serial passaging in vitro. These cells retained their self-renewal potential and were capable of multi-lineage differentiation.

Secondary sphere formation assay

Tumorspheres were dissociated using 5–10 μ L Liberase Blendzyme3 in 1 mL PBS for 5 min at 37 °C. Cells were plated at 200 cells per well in 200 μ L of TSM media in a 96-well plate. Cultures were left undisturbed at 37 °C, 5% CO₂. After four days, the number of secondary spheres per well were counted and used to estimate the mean number of spheres per 2000 cells.

Cell proliferation assay

Single cells were plated in a 96-well plate at a density of 1,000 cells/200 μ L per well in quadruplicate and incubated for five days. 20 μ L of Presto Blue (Invitrogen), a fluorescent cell metabolism indicator, was added to each well approximately 4 h prior to the readout time point. Fluorescence was measured using a FLUOstar Omega Fluorescence 556 Microplate reader (BMG LABTECH) at excitation and emission wavelengths of 535 nm and 600 nm respectively. Readings were analyzed using Omega analysis software.

Viral production and transduction

Lentiviral vectors (CS-H1-shRNA-EF- 1 α -EGFP) expressing shRNA that targets human BMI1 (target sequence: sh-BMI1-1,

5'-CAGATGAAGATAAGAGAAT-3') and luciferase were kind gifts from Dr. Atushi Iwama. Bmi1 overexpression vector was purchased from Genecopoeia. Replication-incompetent lentiviruses were produced by cotransfection of the knockdown vectors/expression vector and packaging vectors pMD2G and psPAX2 in HEK 293FT cells. Viral supernatants were harvested 48 h after transfection, filtered through a 0.45 µm cellulose acetate filter and precipitated with PEGit (System biosciences). The viral pellet was resuspended in 1.0 mL of DMEM F-12 media, aliquoted and stored at -80 °C.

Quantitative real-time–polymerase chain reaction

Total RNA was extracted using a Norgen Total RNA isolation kit and quantified using the NanoDrop Spectrophotometer ND-1000. Complementary DNA was synthesized from 0.5–1 µg RNA by using iScript cDNA Super Mix (Biorad) and a C1000 Thermo Cycler (Bio-Rad) with the following cycle parameters: 5 min at 25 °C, 20 min at 46 °C, 1 min at 95 °C, hold at 4 °C. qRT-PCR was performed by using Perfecta SybrGreen (Quanta Biosciences) and an Opticon Chroma4 instrument (Bio-Rad). Gene expression was quantified by using Opticon software and expression levels were normalized to 28s rRNA expression.

RT-PCR primers

Bmi1 F	5' GGAGGAGGTGAATGATAAAAGAT 3'
Bmi1 R	5' AGGTTCTCCTCATACATGACA 3'
GAPDH F	5' TGCACCACCAACTGCTTAGC 3'
GAPDH R	5' GGCATGGACTGTGGTCATGAG 3'
28 s rRNA F	5' AAGCAGGAGGTGTCAGAAA 3'
28 s rRNA R	5' GTAAACTAACCTGTCTCACG 3'
FSTL1 F	5' TCT GTG CCA ATG TGT TTT GTG GTG 3'
FSTL1 R	5' TGA GGT AGG TCT TGC CAT TAC 3'
ALK F	5' CTT TGA CTT CCC CTG TGA GC 3'
ALK R	5' GCA GCC TCT CCC TTA CCT C 3'
ITGA2 F	5' AGA TGA TTT GGT CAG AAT GGG ATA AG 3'
ITGA2 R	5' TGG GTG GTG TTT CTC AAA GTG T 3'

Flow cytometric analysis and cell sorting

Tumorspheres were dissociated and single cells resuspended in PBS+2 mM EDTA. Cell suspensions were stained with APC-conjugated anti-CD133 or a matched isotype control (Miltenyi) and incubated for 30 min on ice. Samples were run on a MoFlo XDP Cell Sorter (Beckman Coulter). Dead cells were excluded using the viability dye 7AAD. (1:10; Beckman Coulter). Compensation was performed using mouse IgG CompBeads (BD). Expression of CD133

was defined as positive or negative based on the analysis regions set on the isotype control. Cells were sorted into tubes containing 1 mL Neurocult media and small aliquots of each sort tube were re-analysed to determine the purity of the sorted populations. Cells were allowed to equilibrate at 37 °C for a few hours prior to use in experiments.

In vivo GIC intracranial injections and H&E staining of xenograft tumors

Intracranial injections were performed as previously described (2) using each of the following GICs: shLuc, shBmi1, Ctrl OE and Bmi1 OE. Briefly, the appropriate number of live cells (determined by Trypan Blue exclusion) were resuspended in 10 µL of PBS. NOD-SCID mice were anesthetized using isoflurane gas (5% induction, 2.5% maintenance) and cells were injected into the frontal lobe using a 10 µL Hamilton syringe as per REB-approved protocols, in a non-randomized, non-blinded fashion. The mice were sacrificed when the control group reached endpoint. Upon reaching endpoint, brains were harvested, formalin-fixed, and paraffin-embedded for hematoxylin and eosin (H&E) and human COX IV staining (Cell Signalling). Images were captured using an Aperio Slide Scanner and analyzed using ImageScope v11.1.2.760 software (Aperio).

Zone exclusion migration assay

GIC spheres were dissociated to single cells and replated at a density of 30,000 cells per well in a 96 well plate (polyornithine-laminin coated) with a 1% agar drop in the center of the well. After 24 h to allow cell adherence, the agar drop was removed, the wells washed gently with PBS to remove floating cells. Migration into the empty zone was monitored over 3 days, with time points taken at day 0 and day 3.

RNA seq analysis

RNA samples from 3 independent GIC lines that were sorted for CD133 (shLuc or shBMI1) were labelled using Illumina Total Prep-96 RNA Amplification kit (Ambion) as per amplification protocol. 750 ng of cRNA generated from these samples were hybridized onto Human HT-12 V4 Beadchips. The BeadChips were incubated at 58 °C, with rotation speed 5 for 18 h for hybridization. The BeadChips were washed and stained as per Illumina protocol and scanned on the iScan (Illumina). The data files were quantified in GenomeStudio Version 2011.1 (Illumina). All samples passed Illumina sample dependent and independent QC Metrics. GSEA analysis was performed using the MySigDB oncogenic signature collection, and resulted in a set of 556

differential genes (FDR < 0.05) in CD133-positive samples (418 down-regulated and 138 upregulated a set of 427 differential genes (FDR < 0.05) in CD133-negative samples (242 down-regulated and 185 upregulated).

Statistical analysis

Biological replicates from at least three patient samples were compiled for each experiment, unless otherwise specified in figure legends. Respective data represent mean \pm SD, *n* values are listed in figure legends. Student's *t*-test analyses, 2-way ANOVA with Bonferroni post-hoc tests, and Log-rank (Mantel-Cox Test) analysis were performed using GraphPad Prism 5. *P* < 0.05 was considered significant. Statistical tests for in silico analyses were two-sided and were completed in R.

References

- Alkema MJ, Wiegant J, Raap AK et al (1993) Characterization and chromosomal localization of the human proto-oncogene BMI-1. *Hum Mol Genet* 2:1597–1603
- Bracken AP, Dietrich N, Pasini D et al (2006) Genome-wide mapping of Polycomb target genes unravels their roles in cell fate transitions. *Genes Dev* 20:1123–1136. <https://doi.org/10.1101/gad.381706>
- Sauvageau M, Sauvageau G (2010) Polycomb group proteins: multi-faceted regulators of somatic stem cells and cancer. *Cell Stem Cell* 7:299–313. <https://doi.org/10.1016/j.stem.2010.08.002>
- Schuringa JJ, Vellenga E (2010) Role of the polycomb group gene BMI1 in normal and leukemic hematopoietic stem and progenitor cells. *Curr Opin Hematol* 17:294–299. <https://doi.org/10.1097/MOH.0b013e328338c439>
- Valk-Lingbeek ME, Bruggeman SWM, van Lohuizen M (2004) Stem cells and cancer; the polycomb connection. *Cell* 118:409–418. <https://doi.org/10.1016/j.cell.2004.08.005>
- Abdoh M, Facchino S, Chatoo W et al (2009) BMI1 sustains human glioblastoma multiforme stem cell renewal. *J Neurosci* 29:8884–8896. <https://doi.org/10.1523/JNEUROSCI.0968-09.2009>
- Ailles LE, Weissman IL (2007) Cancer stem cells in solid tumors. *Curr Opin Biotechnol* 18:460–466. <https://doi.org/10.1016/j.copbi.2007.10.007>
- Bruggeman SWM, Hulsman D, Tanger E et al (2007) Bmi1 controls tumor development in an Ink4a/Arf-independent manner in a mouse model for glioma. *Cancer Cell* 12:328–341. <https://doi.org/10.1016/j.ccr.2007.08.032>
- Fasano CA, Dimos JT, Ivanova NB et al (2007) shRNA knock-down of Bmi-1 reveals a critical role for p21-Rb pathway in NSC self-renewal during development. *Cell Stem Cell* 1:87–99. <https://doi.org/10.1016/j.stem.2007.04.001>
- Lessard J, Sauvageau G (2003) Bmi-1 determines the proliferative capacity of normal and leukaemic stem cells. *Nature* 423:255–260. <https://doi.org/10.1038/nature01572>
- Park I-K, Morrison SJ, Clarke MF (2004) Bmi1, stem cells, and senescence regulation. *J Clin Invest* 113:175–179. <https://doi.org/10.1172/JCI20800>
- Molofsky AV, Pardal R, Iwashita T et al (2003) Bmi-1 dependence distinguishes neural stem cell self-renewal from progenitor proliferation. *Nature* 425:962–967. <https://doi.org/10.1038/nature02060>
- He S, Iwashita T, Buchstaller J et al (2009) Bmi-1 over-expression in neural stem/progenitor cells increases proliferation and neurogenesis in culture but has little effect on these functions in vivo. *Dev Biol* 328:257–272. <https://doi.org/10.1016/j.ydbio.2009.01.020>
- Yadiri G, Leinster V, Acquati S et al (2011) Conditional activation of Bmi1 expression regulates self-renewal, apoptosis, and differentiation of neural stem/progenitor cells in vitro and in vivo. *Stem Cells Dayt Ohio* 29:700–712. <https://doi.org/10.1002/stem.614>
- Haupt Y, Alexander WS, Barri G et al (1991) Novel zinc finger gene implicated as myc collaborator by retrovirally accelerated lymphomagenesis in E mu-myc transgenic mice. *Cell* 65:753–763
- van Lohuizen M, Verbeek S, Scheijen B et al (1991) Identification of cooperating oncogenes in E mu-myc transgenic mice by provirus tagging. *Cell* 65:737–752
- Chiba T, Miyagi S, Saraya A et al (2008) The polycomb gene product BMI1 contributes to the maintenance of tumor-initiating side population cells in hepatocellular carcinoma. *Cancer Res* 68:7742–7749. <https://doi.org/10.1158/0008-5472.CAN-07-5882>
- Silva J, García JM, Peña C et al (2006) Implication of polycomb members Bmi-1, Mel-18, and Hpc-2 in the regulation of p16INK4a, p14ARF, h-TERT, and c-Myc expression in primary breast carcinomas. *Clin Cancer Res Off J Am Assoc Cancer Res* 12:6929–6936. <https://doi.org/10.1158/1078-0432.CCR-06-0788>
- Leung C, Lingbeek M, Shakhova O et al (2004) Bmi1 is essential for cerebellar development and is overexpressed in human medulloblastomas. *Nature* 428:337–341. <https://doi.org/10.1038/nature02385>
- Jacobs JJ, Kieboom K, Marino S et al (1999) The oncogene and Polycomb-group gene bmi-1 regulates cell proliferation and senescence through the ink4a locus. *Nature* 397:164–168. <https://doi.org/10.1038/16476>
- Liu S, Dontu G, Mantle ID et al (2006) Hedgehog signaling and Bmi-1 regulate self-renewal of normal and malignant human mammary stem cells. *Cancer Res* 66:6063–6071. <https://doi.org/10.1158/0008-5472.CAN-06-0054>
- Wang G, Liu L, Sharma S et al (2012) Bmi-1 confers adaptive radioresistance to KYSE-150R esophageal carcinoma cells. *Biochem Biophys Res Commun* 425:309–314. <https://doi.org/10.1016/j.bbrc.2012.07.087>
- Merve A, Dubuc AM, Zhang X et al (2014) Polycomb group gene BMI1 controls invasion of medulloblastoma cells and inhibits BMP-regulated cell adhesion. *Acta Neuropathol Commun* 2:10. <https://doi.org/10.1186/2051-5960-2-10>
- Shan Z, Tian R, Zhang M, et al (2016) miR128-1 inhibits the growth of glioblastoma multiforme and glioma stem-like cells via targeting BMI1 and E2F3. *Oncotarget* 7:78813–78826. <https://doi.org/10.18632/oncotarget.12385>
- Sugihara H, Ishimoto T, Watanabe M et al (2013) Identification of miR-30e* regulation of Bmi1 expression mediated by tumor-associated macrophages in gastrointestinal cancer. *PLoS ONE* 8:e81839. <https://doi.org/10.1371/journal.pone.0081839>
- Gargiulo G, Cesaroni M, Serresi M et al (2013) In vivo RNAi screen for BMI1 targets identifies TGF- β /BMP-ER stress pathways as key regulators of neural- and malignant glioma-stem cell homeostasis. *Cancer Cell* 23:660–676. <https://doi.org/10.1016/j.ccr.2013.03.030>
- Chowdhury M, Mihara K, Yasunaga S et al (2007) Expression of Polycomb-group (PcG) protein BMI-1 predicts prognosis in patients with acute myeloid leukemia. *Leukemia* 21:1116–1122. <https://doi.org/10.1038/sj.leu.2404623>
- Wu Z, Wang Q, Wang L et al (2013) Combined aberrant expression of Bmi1 and EZH2 is predictive of poor prognosis

- in glioma patients. *J Neurol Sci* 335:191–196. <https://doi.org/10.1016/j.jns.2013.09.030>
29. Glinsky GV, Berezovska O, Glinskii AB (2005) Microarray analysis identifies a death-from-cancer signature predicting therapy failure in patients with multiple types of cancer. *J Clin Invest* 115:1503–1521. <https://doi.org/10.1172/JCI23412>
 30. Bao S, Wu Q, McLendon RE et al (2006) Glioma stem cells promote radioresistance by preferential activation of the DNA damage response. *Nature* 444:756–760. <https://doi.org/10.1038/nature05236>
 31. Qazi MA, Vora P, Venugopal C et al (2016) A novel stem cell culture model of recurrent glioblastoma. *J Neurooncol* 126:57–67. <https://doi.org/10.1007/s11060-015-1951-6>
 32. Facchino S, Abdouh M, Chatoo W, Bernier G (2010) BMI1 confers radioresistance to normal and cancerous neural stem cells through recruitment of the DNA damage response machinery. *J Neurosci Off J Soc Neurosci* 30:10096–10111. <https://doi.org/10.1523/JNEUROSCI.1634-10.2010>
 33. Singh SK, Hawkins C, Clarke ID et al (2004) Identification of human brain tumour initiating cells. *Nature* 432:396–401. <https://doi.org/10.1038/nature03128>
 34. Michael LE, Westerman BA, Ermilov AN et al (2008) Bmi1 is required for hedgehog pathway-driven medulloblastoma expansion. *Neoplasia* 10:1343–1349
 35. Dovey JS, Zacharek SJ, Kim CF, Lees JA (2008) Bmi1 is critical for lung tumorigenesis and bronchioalveolar stem cell expansion. *Proc Natl Acad Sci USA* 105:11857–11862. <https://doi.org/10.1073/pnas.0803574105>
 36. Agnihotri S, Munoz D, Zadeh G, Guha A (2011) Brain tumor-initiating cells and cells of origin in glioblastoma. *Transl Neurosci* 2:331–338. <https://doi.org/10.2478/s13380-011-0037-y>
 37. Venugopal C, Li N, Wang X et al (2012) Bmi1 marks intermediate precursors during differentiation of human brain tumor initiating cells. *Stem Cell Res* 8:141–153. <https://doi.org/10.1016/j.scr.2011.09.008>
 38. Chen D, Wu M, Li Y et al (2017) Targeting BMI1+ Cancer Stem Cells Overcomes Chemoresistance and Inhibits Metastases in Squamous Cell Carcinoma. *Cell Stem Cell* 20:621.e6–634.e6. <https://doi.org/10.1016/j.stem.2017.02.003>
 39. Liu G, Yuan X, Zeng Z et al (2006) Analysis of gene expression and chemoresistance of CD133+ cancer stem cells in glioblastoma. *Mol Cancer* 5:67. <https://doi.org/10.1186/1476-4598-5-67>
 40. de Almeida SF, Lunardi Brunetto A, Schwartzmann G et al (2012) Glioma revisited: from neurogenesis and cancer stem cells to the epigenetic regulation of the niche. *J Oncol* 2012:537861. <https://doi.org/10.1155/2012/537861>
 41. Kong Y, Ai C, Dong F et al (2018) Targeting of BMI-1 with PTC-209 inhibits glioblastoma development. *Cell Cycle Georget Tex*. <https://doi.org/10.1080/15384101.2018.1469872>
 42. Badodi S, Dubuc A, Zhang X et al (2017) Convergence of BMI1 and CHD7 on ERK signaling in medulloblastoma. *Cell Rep* 21:2772–2784. <https://doi.org/10.1016/j.celrep.2017.11.021>
 43. Cao R, Wang L, Wang H et al (2002) Role of histone H3 lysine 27 methylation in polycomb-group silencing. *Science* 298:1039–1043. <https://doi.org/10.1126/science.1076997>
 44. Filbin MG, Tirosh I, Hovestadt V et al (2018) Developmental and oncogenic programs in H3K27M gliomas dissected by single-cell RNA-seq. *Science* 360:331–335. <https://doi.org/10.1126/science.aao4750>
 45. Jin X, Kim LJY, Wu Q et al (2017) Targeting glioma stem cells through combined BMI1 and EZH2 inhibition. *Nat Med* 23:1352–1361. <https://doi.org/10.1038/nm.4415>
 46. Liu P-P, Tang G-B, Xu Y-J et al (2017) MiR-203 interplays with polycomb repressive complexes to regulate the proliferation of neural stem/progenitor cells. *Stem Cell Rep* 9:190–202. <https://doi.org/10.1016/j.stemcr.2017.05.007>
 47. Cannon CE, Titchenell PM, Groff DN et al (2014) The Polycomb protein, Bmi1, regulates insulin sensitivity. *Mol Metab* 3:794–802. <https://doi.org/10.1016/j.molmet.2014.08.002>
 48. Sanzey M, Abdul Rahim SA, Oudin A et al (2015) Comprehensive analysis of glycolytic enzymes as therapeutic targets in the treatment of glioblastoma. *PLoS ONE* 10:e0123544. <https://doi.org/10.1371/journal.pone.0123544>
 49. Koren A, Rijavec M, Kern I et al (2016) BMI1, ALDH1A1, and CD133 transcripts connect epithelial-mesenchymal transition to cancer stem cells in lung carcinoma. *Stem Cells Int* 2016:9714315. <https://doi.org/10.1155/2016/9714315>
 50. Verhaak RGW, Hoadley KA, Purdom E et al (2010) Integrated genomic analysis identifies clinically relevant subtypes of glioblastoma characterized by abnormalities in PDGFRA, IDH1, EGFR, and NF1. *Cancer Cell* 17:98–110. <https://doi.org/10.1016/j.ccr.2009.12.020>
 51. Zarkoob H, Taube JH, Singh SK et al (2013) Investigating the link between molecular subtypes of glioblastoma, epithelial-mesenchymal transition, and CD133 cell surface protein. *PLoS ONE* 8:e64169. <https://doi.org/10.1371/journal.pone.0064169>
 52. Morris SW, Kirstein MN, Valentine MB et al (1994) Fusion of a kinase gene, ALK, to a nucleolar protein gene, NPM, in non-Hodgkin's lymphoma. *Science* 263:1281–1284
 53. Soda M, Choi YL, Enomoto M et al (2007) Identification of the transforming EML4-ALK fusion gene in non-small-cell lung cancer. *Nature* 448:561–566. <https://doi.org/10.1038/nature05945>
 54. Kalamatianos T, Denekou D, Stranjalis G, Papadimitriou E (2018) Anaplastic lymphoma kinase in glioblastoma: detection/diagnostic methods and therapeutic options. *Recent Patents Anticancer Drug Discov* 13:209–223. <https://doi.org/10.2174/1574892813666180115151554>
 55. Reddy SP, Britto R, Vinnakota K et al (2008) Novel glioblastoma markers with diagnostic and prognostic value identified through transcriptome analysis. *Clin Cancer Res* 14:2978–2987. <https://doi.org/10.1158/1078-0432.CCR-07-4821>
 56. Jin X, Nie E, Zhou X et al (2017) Fstl1 Promotes glioma growth through the BMP4/Smad1/5/8 signaling pathway. *Cell Physiol Biochem* 44:1616–1628. <https://doi.org/10.1159/000485759>
 57. Ding W, Fan X-L, Xu X et al (2015) Epigenetic silencing of ITGA2 by MiR-373 promotes cell migration in breast cancer. *PLoS ONE* 10:e0135128. <https://doi.org/10.1371/journal.pone.0135128>
 58. Ferraro A, Boni T, Pintzas A (2014) EZH2 regulates cofilin activity and colon cancer cell migration by targeting ITGA2 gene. *PLoS ONE* 9:e115276. <https://doi.org/10.1371/journal.pone.0115276>
 59. Osuka S, Van Meir EG (2017) Overcoming therapeutic resistance in glioblastoma: the way forward. *J Clin Invest* 127:415–426. <https://doi.org/10.1172/JCI89587>
 60. Gardeck AM, Sheehan J, Low WC (2017) Immune and viral therapies for malignant primary brain tumors. *Expert Opin Biol Ther* 17:457–474. <https://doi.org/10.1080/14712598.2017.1296132>
 61. Rooj AK, Ricklefs F, Mineo M et al (2017) MicroRNA-mediated dynamic bidirectional shift between the subclasses of glioblastoma stem-like cells. *Cell Rep* 19:2026–2032. <https://doi.org/10.1016/j.celrep.2017.05.040>

Publisher's Note Springer Nature remains neutral with regard to jurisdictional claims in published maps and institutional affiliations.